water

MDPI

Article

Origin and Hydrogeochemical Evolution of Jety-Oguz Mineral Waters (Issyk-Kul Basin, Tien Shan)

Ekaterina I. Baranovskaya [1,*], Natalia A. Kharitonova [1], George A. Chelnokov [2], Farid S. Salikhov [3] and Irina A. Tarasenko [4]

[1] Faculty of Geology, Lomonosov Moscow State University, GSP-1, Leninskiye Gory, 119991 Moscow, Russia; tchenat@mail.ru
[2] Heat and Mass Transfer Laboratory, Geological Institute Russian Academy of Science, Pyzhevsky Lane 7, Bld. 1, 119017 Moscow, Russia; geowater@mail.ru
[3] Department of Mathematics and Natural Sciences, Branch of Lomonosov Moscow State University, Dushanbe 734003, Tajikistan; ffaarriidd@bk.ru
[4] Laboratory of Hypergene Processes Geochemistry, Far East Geological Institute, Far Eastern Branch Russian Academy of Science, Prospect 100-Letya 159, 690022 Vladivostok, Russia; tarasenko_irina@mail.ru
* Correspondence: baranovskaya_kat@mail.ru; Tel.: +7-968-671-4199

Abstract

This article presents a comprehensive study of the nitrogen-radon thermal mineral waters of the Jety-Oguz area, located in the southeastern part of the Issyk-Kul intermountain artesian basin (Northern Tien Shan). Based on new data from chemical and isotopic ($\delta^{18}O$, δD) analyses of natural waters (lake, river, and mineral) and the chemical composition of the water-bearing rocks, we identify the formation mechanisms of mineral waters with diverse composition, total dissolved solids (TDS), and temperature. Three main genetic types have been identified: (1) saline, high-TDS (up to 12.8 g/L) chloride sodium-calcium thermal waters (up to 32 °C). These waters are of meteoric origin and circulate within Middle Carboniferous carbonate rocks, acquiring their unique composition at depths of up to 3.0 km, where reservoir temperatures reach ~105 °C; (2) chloride-sulfate sodium-calcium waters (0.5 g/L, fresh, 22 °C), formed in alluvial deposits within the zone of active water exchange; and (3) low-TDS (1.8 g/L, brackish) waters of mixed composition, resulting from the mixing of a deep fluid with infiltrating meteoric waters. Isotopic data confirm a meteoric origin for all studied waters, including the high-TDS thermal types. The chemical composition diversity is attributed to several processes: mixing between the deep, high-TDS fluid and low-TDS infiltration waters, intense dissolution of evaporite rocks, and water–rock interaction. These findings are crucial for understanding the genesis of mineral waters in the Tien Shan intermountain basins and provide a scientific basis for their sustainable balneological exploitation.

Keywords: thermal mineral waters; chemical composition; stable isotopes ($\delta^{18}O$; δD); intermountain artesian basins; Jety-Oguz; Issyk-Kul; Northern Tien Shan

Academic Editors: Tianming Huang, Zhonghe Pang, Buli Cui, Jinlong Zhou, Xianjun Xie and Zhongyin Cai

Received: 19 November 2025
Revised: 20 December 2025
Accepted: 23 December 2025
Published: 26 December 2025

Copyright: © 2025 by the authors. Licensee MDPI, Basel, Switzerland. This article is an open access article distributed under the terms and conditions of the Creative Commons Attribution (CC BY) license.

1. Introduction

The Northern Tien Shan region, specifically within the Issyk-Kul intermountain artesian basin, hosts over 100 natural discharges of mineral waters. These waters exhibit a wide range of total dissolved solids (TDS), temperatures, gas and ionic compositions, and specific components. They are primarily concentrated in the mountainous areas, where

complex geological and hydrogeological conditions drive diverse formation mechanisms. The Issyk-Kul Depression, bounded by the Kyungey-Ala-Too Range to the north and the Terskey-Ala-Too Range to the south (with peak elevations exceeding 5.200 m), is a Late Cenozoic intermontane basin. It developed within the North Tian Shan Caledonian fold system and is filled with Meso-Cenozoic continental molasse-type sedimentary rocks, reaching thicknesses of up to 5.0 km. The surrounding ranges are composed of a complex of Proterozoic and Paleozoic rocks [1,2]. The combination of favorable climatic and landscape conditions with this diversity of mineral water types creates a unique balneological potential in the region, which fosters the development of spa and resort infrastructure.

The northern slope of the Terskey-Ala-Too ridge hosts several occurrences of nitrogenous low-TDS thermal waters, including the springs of Jety-Oguz, Bozuchuk, Ak-Suu, Altyn-Arasan, Chon-Kyzyl-Su, Juukuchak, and Aitor, which together form the Karakol thermal zone [3,4]. Among these, the Jety-Oguz mineral waters are distinguished by their elevated TDS.

These waters are of considerable scientific and practical interest due to their balneological properties and potential use for therapeutic, domestic purposes. Despite previous studies focusing on chemical of groundwater in the Issyk-Kul basin, there is still limited understanding of the formation conditions, circulation depths, and geochemical processes controlling the hydrochemical diversity of the Jety-Oguz mineral waters.

This article investigates the genesis of the solute composition and the formation conditions of the unique Jety-Oguz nitrogen-radon thermal waters, located in the southeastern part of the Issyk-Kul intermountain artesian basin.

The mineral waters of the Jety-Oguz area are notable for their distinctive chemical composition and valuable therapeutic properties. Known since ancient times, these mineral waters have been utilized for over a century [3]. A remarkable feature of this area is the significant variability in water TDS, temperature, and radioactivity observed over a relatively small surface area and within narrow depth intervals.

The radon found in groundwater originates from the radioactive decay of uranium and thorium in the granitic and metamorphic basement rocks of the Terskey-Ala-Too Range. As noted by [4], radon enters the aquifers mainly through fracture zones and tectonic faults. In these structures, groundwater becomes enriched in radium due to leaching of granitoid rocks. Additional enrichment takes place in the discharge areas. When thermal waters mix with colder fresh groundwater, calcium carbonate precipitates. This carbonate material sorbs radium and forms small "emanation collectors" at the discharge points, which then supply extra radon to the mineral waters. Balneological data show that the radon activity in the springs corresponds to low- to medium-radon waters, typically around 20–40 nCi/L.

The mineral water discharges are concentrated along the right bank of the eponymous Jety-Oguz River, where a sanatorium is located. The high-TDS waters are used topically in bath therapies for treating musculoskeletal, neurological, and gynecological conditions. Waters of medium TDS from a drinking fountain are utilized for oral administration in cases of chronic digestive disorders. From a therapeutic standpoint, the radioactive, high-TDS thermal waters are of particular interest and are effectively employed for balneotherapy.

Understanding the formation of the Jety-Oguz mineral waters is critical for elucidating the chemical transformation mechanisms of thermal fluids within the intermountain basins of the Northern Tien Shan, while also providing a scientific basis for their sustainable therapeutic use. Despite extensive research on the Jety-Oguz waters by various researchers [3–7], the genesis of the high-TDS thermal waters in the southeastern Issyk-Kul artesian basin remains a subject of ongoing scientific debate.

https://doi.org/10.3390/w18010075

This article presents new chemical and isotopic ($\delta^{18}O$, δD) data for natural waters (surface, fresh groundwater, mineral waters) from the Jety-Oguz area, along with the mineralogical and chemical composition of the water-bearing rocks.

2. Study Area

The Jety-Oguz area is situated in the southeastern part of the Issyk-Kul intermountain artesian basin [1], at an elevation of approximately 2050 m above sea level. It lies 25–30 km south of Lake Issyk-Kul and a similar distance from the regional administrative center, Karakol.

The area's topography is characterized by deep erosional dissection and pronounced altitudinal zonation, with absolute elevations increasing southward towards the northern slope of the Terskey-Ala-Too range (Figure 1). Precipitation is unevenly distributed across the basin, with mean annual values ranging from 100–250 mm/year in the west, 400–450 mm/year in the central part, to 600–900 mm/year in the southeast.

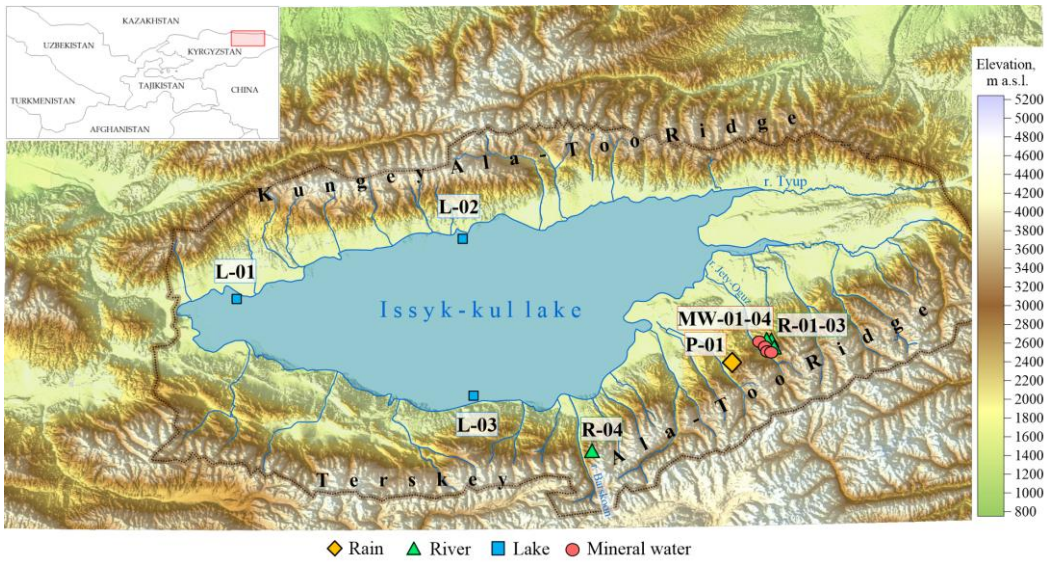


Figure 1. Location of the study area and sampling points in the Jety-Oguz area (Issyk-Kul basin, Tien Shan).

The density of the river network and its discharge reach their maximum in the southeastern part of the basin. The area is drained by the Jety-Oguz River and its tributaries. In its upper reaches, the river flows through a narrow gorge incised into Paleozoic rocks with steep, rocky banks. Further downstream, within the zone of Meso-Cenozoic deposits, the valley widens, and this is where the eponymous resort is located. The northern boundary of the area is marked by an escarpment composed of brick-red Paleogene conglomerates, a local landmark known as the "Seven Bulls" (which translates into Kyrgyz as Jety-Oguz).

The central part of the Issyk-Kul basin is occupied by the deep, endorheic Lake Issyk-Kul. The lake fills a latitudinally elongated tectonic depression at an altitude of 1609 m above sea level. Its catchment area exceeds 22,000 km^2, with a maximum depth of 668 m (average depth 278 m) [1]. The coastal zone is a foothill plain, 2 to 20 km wide, formed by alluvial fans of mountain rivers; this is where the main urban settlements and resort infrastructure of the region are concentrated. The primary water input to the lake comes from rivers originating in the high-altitude glacial zone.

Geologically, the Issyk-Kul depression is a major feature of the Northern Tien Shan, filled with a thick sequence (up to 5.0 km) of Meso-Cenozoic continental sediments overlying a folded Lower Paleozoic basement. The lower part of this sequence consists of Jurassic coal-bearing deposits (up to 10 m thick), including clays, siltstones, and sandstones

with coal interbeds. These are overlain by gravelites, conglomerates, and sandstones (up to 60 m), which are in turn covered by a 550–1500 m thick layer of continental sediments comprising clays, sandstones, gravelites, and breccias. The uppermost part of the sequence consists of Neogene-Quaternary coarse-grained alluvial-proluvial deposits exceeding 2000 m in thickness [4].

The recharge areas for the basin are located in the high-altitude axial zones of the surrounding ranges (4500–5000 m a.s.l.), where Paleozoic and Precambrian magmatic, metamorphic, and sedimentary rocks are exposed. Here, atmospheric precipitation actively infiltrates, creating favorable conditions for the formation of deep groundwater flow. Fault systems drain the aquifer complexes, creating both local and regional discharge zones. In the marginal parts of the basin, the intensely dissected topography and well-developed fracture systems facilitate rock leaching by infiltrating waters. Groundwater discharge is associated with the faults that bound the lake basin, as well as with the articulation zones between the depression and the surrounding ranges.

The western part of the Issyk-Kul basin is characterized by a gentle subsidence, while its eastern part is significantly downwarped towards the Paleozoic basement. The Jety-Oguz thermal water area is located in the zone where the southeastern part of the basin articulates with the Terskey-Ala-Too anticlinorium.

The monoclinal dip of the rocks in the southeastern part of the basin is complicated by secondary brachyanticlinal fold structures, in whose crests older rocks are exposed from beneath the Cenozoic cover. One such structure, to which the Jety-Oguz mineral waters are confined, is the Jety-Oguz anticline. The fold's core is composed of Proterozoic schists and granites, while its limbs contain Middle Carboniferous limestones, sandstones, and siltstones, Jurassic conglomerates, and Paleogene-Neogene sandy-clay deposits [3,4].

Faulting is widespread in the Issyk-Kul Depression, particularly in its marginal parts. The largest is the regional Karakol Thrust, which places Early Caledonian granites over red-colored Paleogene sediments and trends northeast [4]. The Jety-Oguz area is also affected by smaller-scale discontinuities (Figure 2).

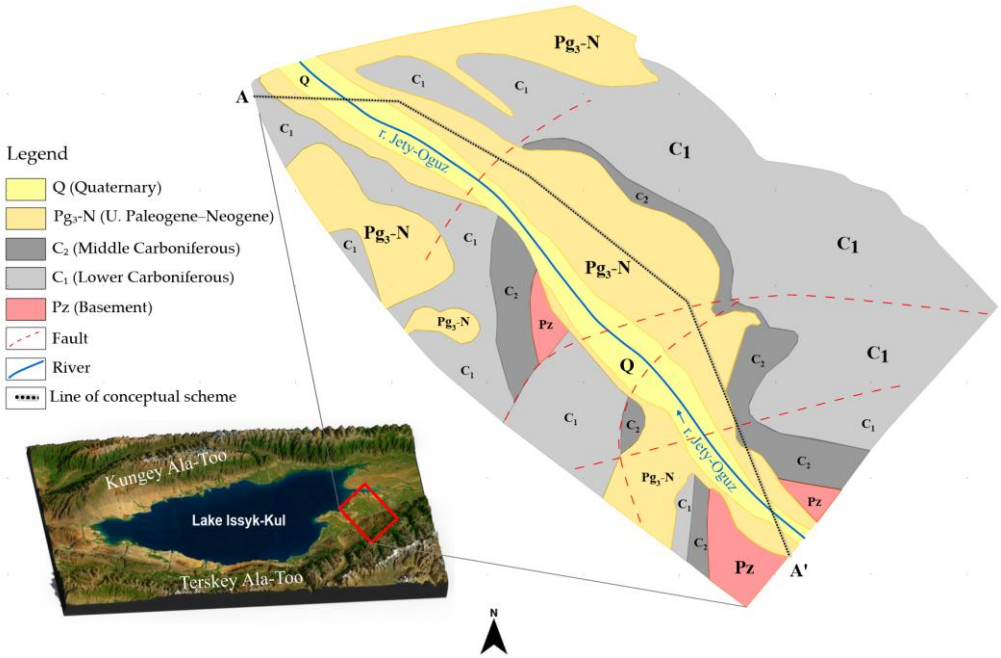


Figure 2. Schematic geological map of the Jety-Oguz area. The map shows the distribution of Quaternary (Q) alluvial-proluvial deposits; Upper Paleogene-Neogene (Pg_3-N) brick-red clays; Middle Carboniferous (C_2) fractured limestones overlying Lower Carboniferous (C_1) sandstones and shales; Precambrian metamorphic basement (Pz) of schists, quartzites, and gneisses.

https://doi.org/10.3390/w18010075

The hydrogeological conditions of the Jety-Oguz area are determined by its position on the northern slope of the Terskey-Ala-Too range, which acts as a recharge area characterized by intensive water exchange. Where fractured Precambrian and Paleozoic metamorphic, magmatic, and sedimentary rocks are exposed, conditions are favorable for the infiltration of abundant precipitation and the accumulation of significant groundwater reserves. Further downslope, the Paleozoic rocks are overlain by a thick sequence of Meso-Cenozoic sediments, where confined (artesian) conditions develop. However, the presence of the Jety-Oguz brachyanticline disrupts this typical hydrogeological section, as Paleozoic rocks are exposed in its crest, creating a localized area of additional recharge and discharge.

The highest hydraulic conductivity is associated with Carboniferous limestones, which contain both regional and local fracture zones. The main groundwater discharge area is linked to the erosional incision of the Jety-Oguz River, where the carbonate rocks are exposed at the surface and the contact between Paleozoic and Meso-Cenozoic sediments reaches its lowest elevation. The mineral waters discharge on the right bank of the Jety-Oguz River, emerging from Middle Carboniferous carbonate rocks in the northern limb of the anticline [3].

Thus, the hydrogeology of the Jety-Oguz area is strongly controlled by the brachyanticline structure, which serves as a primary discharge zone for the mineral waters. Intense fracturing in Carboniferous limestones and surrounding rocks provides high hydraulic conductivity, promoting the ascent of deep fluids to the surface. The area's climate and precipitation patterns play a key role in water recharge. This combination of structural, lithological, and climatic factors results in diverse hydrogeochemical environments, ranging from shallow active water exchange zones in alluvial deposits to deep thermal reservoirs within sedimentary rocks.

3. Materials and Methods

This study is based on field research conducted in the Issyk-Kul region of the Kyrgyz Republic during 2023–2024. Building upon the regional hydrogeochemical framework established for the entire Issyk-Kul basin [1], this paper presents a detailed case study of the Jety-Oguz mineral water area, located in its southeastern part. The dataset for this focused investigation comprises 11 water samples from the Jety-Oguz area, including 3 lake (L-01–L-03), 4 river and streams (R01–R04), and 4 groundwater (MW-01–MW-04) samples, as well as atmospheric precipitation (P-01). The collected water samples were subjected to a comprehensive analysis, including their chemical and stable isotope (oxygen and hydrogen) composition. The sampling locations are presented in (Figure 1).

In situ measurements of unstable parameters (temperature, pH) were performed using a portable analyzer (Milwaukee Instruments Inc., Rocky Mount, NC, USA). Bicarbonate (HCO_3^-) was determined on-site by titration. Water samples intended for laboratory chemical analysis were filtered in the field through 0.45 μm cellulose filters and preserved according to standard protocols: samples for cation and trace element analysis were acidified with ultrapure HNO_3 to pH < 2, while samples for anion analysis were left unacidified.

Major cation and anion concentrations were determined by ion chromatography using an LC-20 liquid chromatograph (Shimadzu, Kyoto, Japan). The analytical precision for major ions is typically better than ±5%. Organic carbon content was analyzed by infrared detection on a TOC-V analyzer (Shimadzu, Kyoto, Japan) at the analytical laboratory of the Far Eastern Branch of the Russian Academy of Sciences (FEB RAS).

https://doi.org/10.3390/w18010075

The trace element composition was determined using inductively coupled plasma mass spectrometry (ICP-MS) on an Agilent 7700 mass spectrometer (Agilent Technologies, Santa Clara, CA, USA) at the FEB RAS analytical laboratory. The detection limits for most trace elements were better than 0.1 ppb (μg/L).

The stable isotope composition of natural waters ($\delta^{18}O$ and δD) was analyzed using a Picarro laser absorption spectrometer (Santa Clara, CA, USA) at the analytical laboratory of the Geophysical Institute of the Russian Academy of Sciences (GIN RAS). The measurement precision, based on repeated analysis of internal laboratory standards, was ±0.1 ‰ for $\delta^{18}O$ and ±1.0 ‰ for δD. The $\delta^{18}O$ and δD results are reported relative to the V-SMOW standard [8].

To characterize the water-bearing rocks and secondary phase within the Jety-Oguz area, five representative rock samples were collected and analyzed.

The major element composition of host rock samples was determined by inductively coupled plasma atomic emission spectrometry (ICP-AES) on an iCAP 7600 Duo spectrometer (Thermo Fisher Scientific, Waltham, MA, USA) and by inductively coupled plasma mass spectrometry (ICP-MS) on an Agilent 8800 spectrometer (Agilent Technologies, Santa Clara, CA, USA). The analytical accuracy was verified using international rock reference standards (e.g., SCo-1) and is generally within ±5% for major oxides. The content of H_2O, loss on ignition (LOI), and SiO_2 was determined by gravimetric methods at the FEB RAS analytical chemistry laboratory.

The mineral composition and structural features of the rocks were investigated using light microscopy. Petrographic descriptions were performed with an Amplival polarizing microscope (Carl Zeiss Jena, Jena, Germany) in transmitted light. The analysis aimed to determine the mineralogy and rock type, mineral interrelationships, and evidence of alteration and secondary mineralization.

Mineral saturation indices (SI) were calculated by geochemical modeling using The Geochemist's Workbench (GWB, Community Edition 2021) software [9]. The SI is defined as log (IAP/K_t), where IAP is the ion activity product and K_t is the thermodynamic solubility product at the sample temperature. In this convention, $SI < 0$ indicates undersaturation (potential for dissolution), $SI \approx 0$ indicates equilibrium, and $SI > 0$ indicates oversaturation (potential for precipitation).

Cation and solute geothermometers, based on chemical equilibrium reactions in the water-mineral system, were applied to estimate the reservoir temperatures of the thermal mineral waters [10–17]. To estimate reservoir temperatures, several classical geothermometers were applied: cation geothermometers Na-K [15], K-Mg [11], Mg-Li [17], Na-K-Ca [16] and the silica geothermometer (SiO_2, quartz) [14]. The reliability of cation geothermometers was assessed using the Giggenbach Na-K-Mg ternary diagram [11], which classifies waters into mature (fully equilibrated) and immature (actively circulating) types.

A binary mixing model using conservative tracers (chloride ion, TDS) and isotopic composition ($\delta^{18}O$) was employed to quantitatively assess the mixing proportions in the waters, in accordance with standard methodologies [18].

The circulation depth of the groundwater was estimated based on the regional geothermal gradient [4,6,7,19,20].

The intensity of chemical element migration and their relative mobility were evaluated using the aqueous migration coefficient (Kx) proposed by A.I. Perelman [21].

4. Results

Surface waters in the study area were sampled, including Lake Issyk-Kul (samples L-01 to L-03), a stream in the Jety-Oguz resort area (R-01), a stream in the Jety-Oguz area (R-02), the Jety-Oguz River (R-03), the Barskoon River (R-04), and mineral waters (Figure

1). The chemical composition, TDS, temperature, and pH of the sampled waters are presented in Table 1.

https://doi.org/10.3390/w18010075

Table 1. Chemical composition of the studied water samples.

ID	Type of Water Source	*T* (°C)	pH	TDS (g/L)	Hydrochemical Type	K^+	Na^+	Ca^{2+}	Mg^{2+}	SO_4^{2-}	HCO_3^-	Cl^-	NO_2^-	NO_3^-	NH_4^+	TOC	TC	IC
						Units (mg/L)												
L-01	Lake	13.7	8.7	5.6	Na-Mg-Cl-SO_4	48.2	1204.0	101.0	264.0	2035.0	427.1	1531.0	0.5	0.1	0.1	4.6	70.6	66.0
L-02	Lake	13.5	8.6	5.9	Na-Mg-Cl-SO_4	50.5	1304.0	106.0	279.0	2118.0	398.3	1609.0	0.5	0.1	0.1	1.7	66.5	64.8
L-03	Lake	14.0	8.7	5.9	Na-Cl-SO_4	29.6	1348.0	150.0	250.0	2072.0	405.0	1642.0	0.1	0.1	73.4	2.7	64.5	61.8
R-01	River	14.0	8.6	0.2	Ca-Na-Cl-HCO_3	1.1	22.4	35.5	2.6	20.1	88.5	61.7	0.5	2.7	0.1	0.7	13.7	13.0
R-02	River	9.0	6.0	0.1	Ca-HCO_3	0.9	3.6	44.1	5.1	7.2	97.9	1.2	0.1	2.1	0.2	0.0	32.1	32.2
R-03	River	14.0	5.8	0.1	Ca-HCO_3	0.6	2.0	23.2	3.1	15.8	93.1	2.2	0.1	2.2	0.2	0.2	16.1	15.9
R-04	River	11.0	6.4	0.2	Ca-HCO_3-SO_4	0.5	1.9	32.7	6.6	40.5	94.0	1.3	0.1	2.0	0.1	0.7	18.5	17.8
MW-01	Spring (well)	32.0	7.7	12.8	Na-Ca-Cl	48.4	2605.0	2005.0	3.4	565.0	39.7	7517.0	0.5	3.2	0.1	0.1	6.1	6.1
MW-02	Spring (well)	22.0	9.2	0.5	Na-Ca-Cl-SO_4	2.4	129.0	49.0	0.3	132.0	30.5	158.0	0.5	0.1	0.1	0.8	15.7	14.9
MW-03	Spring (well)	22.0	6.5	0.5	Na-Ca-Cl-SO_4	2.2	116.7	43.9	0.2	129.0	45.3	150.0	0.1	0.1	6.6	0.1	15.4	15.4
MW-04	Spring	17.9	8.5	1.8	Na-Ca-Cl-SO_4	5.9	412.7	221.3	0.6	367.0	42.7	783.0	0.5	0.7	0.1	0.1	5.6	5.6

https://doi.org/10.3390/w18010075

4.1. Surface Water Hydrogeochemistry

The thermal regime of *Lake Issyk-Kul* is primarily determined by its depth. In winter, the surface water layers (down to 100 m) reach temperatures of approximately 5.0 °C, while at depths of 500–600 m, temperatures range from 3.6 to 4.2 °C. During summer (July-August), the temperature of the upper layers reaches 18–20 °C. Based on our sampling in June 2023 and 2024 (L-01–L-03), the average water temperature of Lake Issyk-Kul was 13.7 °C (Table 1). The lake waters are alkaline, with pH values of 8.6–8.7. The TDS of Lake Issyk-Kul was reported as 5.97 g/L [7], which is consistent with our 2023–2024 measurements averaging 5.8 g/L (Table 1). Chemically, the lake water is of the Cl-SO_4—Na-Mg type (Figure 3). The cation ratio (predominance of Na and Mg) is similar to oceanic water, while the anion predominance (Cl and SO_4) is more characteristic of continental lakes [22].

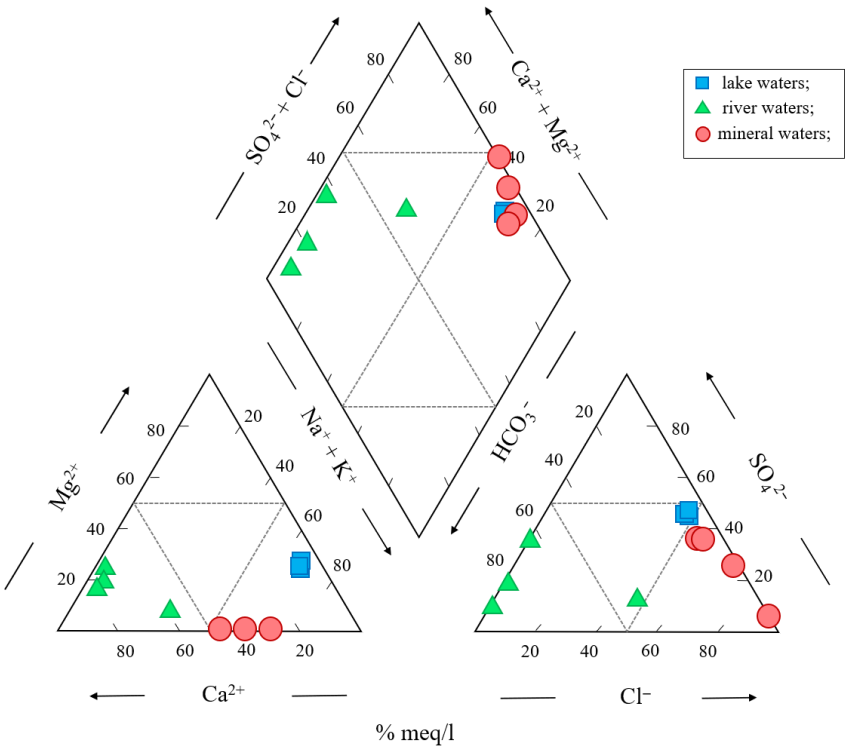


Figure 3. Piper diagram for surface and groundwater samples from the Jety-Oguz area.

The total organic carbon (TOC) content in the sampled lake waters is low, ranging from 1.7 to 4.6 mg/L, with a mean value of 3.0 mg/L (Table 1). However, sample L-03 exhibited an anomalously high ammonium ion (NH_4^+) concentration of 73.4 mg/L. This value significantly exceeds the Russian standard for fishery waters [23] (0.2 mg/L) by a factor of 367 and the EU standard [24] (1.5 mg/L) by a factor of 49.

Elevated nitrite (NO_2^-) concentrations (0.5 mg/L) were also detected in samples L-01 and L-02, exceeding both the Russian regulatory limit for fishery waters (0.26 mg/L) and the EU standard (0.03 mg/L). In sample L-03, the NO_2^- content was lower (0.05 mg/L) but still above the European standard. These exceedances may indicate a localized source of contamination, potentially from wastewater or agricultural fertilizers.

River waters in the southeastern part of the Issyk-Kul basin include small streams flowing through the Jety-Oguz resort area and larger mountain rivers (Jety-Oguz, Barskoon). The temperature of these waters ranged from 9.0 to 14.0 °C (samples R-01 to R-04), with pH values varying from slightly acidic to alkaline (5.8 to 8.6). Alkaline conditions

were observed in the stream within the Jety-Oguz resort (R-01), while the other watercourses were slightly acidic (pH 5.8–6.4) (Table 1).

The TDS of the river waters (0.1–0.2 g/L) is significantly lower than that of Lake Issyk-Kul, which is typical for mountain river systems. The ionic composition of the stream in the resort area (R-01) is of the Cl–HCO_3–Ca–Na hydrochemical type, while the other watercourses are of the HCO_3–Ca (R-02, R-03) and HCO_3–SO_4–Ca (R-04) types (Figure 3).

The anion composition of the river waters is dominated by bicarbonates (64–90% meq), with sulfates contributing up to 35% meq in the Barskoon River (R-04). Sample R-01 is distinctive for its high chloride content (48% meq). Calcium is the dominant cation in all river waters (59–76% meq), followed by magnesium (15–24% meq), with the exception of stream R-01, where sodium is the secondary cation (34% meq).

The TOC content in the river waters is low, varying from 0.01 to 0.7 mg/L (Table 1, Figure 4). Ammonium ion (NH_4^+) concentrations range from 0.1 to 0.22 mg/L. The value in sample R-02 (0.22 mg/L) slightly exceeds the Russian fishery standard (0.2 mg/L) but remains below the EU standard (1.5 mg/L). Nitrite (NO_2^-) concentrations are 0.1 mg/L in most samples, but reach 0.5 mg/L in sample R-01, exceeding both the Russian regulatory limit (0.26 mg/L) and the EU standard (0.03 mg/L) [24].

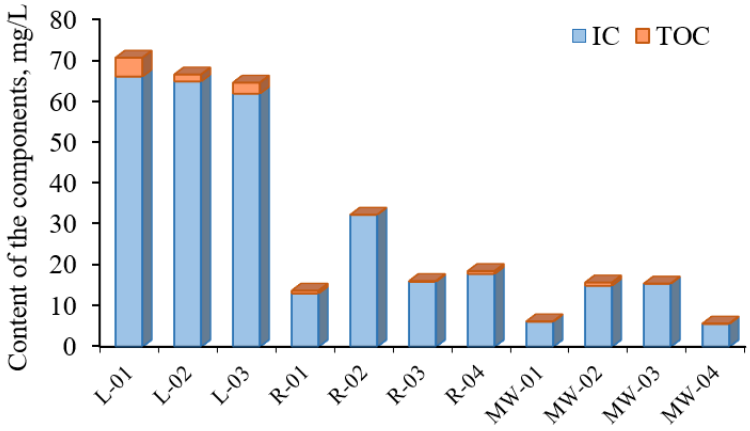


Figure 4. Distribution of carbon species (TC, TOC, IC) in water samples from the Jety-Oguz area.

In summary, the river waters of the southeastern Issyk-Kul basin are characterized by low TDS and a diverse ionic composition dominated by bicarbonates and calcium. The exceptions are samples from within the Jety-Oguz resort (R-01), which show elevated chloride and sulfate levels, suggesting anthropogenic influence.

4.2. Mineral Waters Hydrogeochemistry

The natural mineral waters of the Jety-Oguz area exhibit significant diversity in chemical composition, total dissolved solids (TDS), and temperature, resulting from the complex geological structure and specific hydrogeological conditions of the area.

The discharge temperature of the waters ranges from 17.9 to 32.0 °C (Table 1). According to standard classifications [25,26], water at 17.9 °C is classified as cold (<20 °C), while waters between 22.0 and 32.0 °C are classified as warm. The minimum temperature (17.9 °C) was recorded at a spring (MW-04) draining metamorphic rocks of the Paleozoic basement. The maximum temperature (32.0 °C) is characteristic of water from the well at the Jety-Oguz resort (MW-01), which taps into Carboniferous carbonate deposits.

The pH of the studied mineral waters varies from slightly acidic (6.5 in MW-03) to alkaline (9.2 in MW-02), reflecting differing hydrogeochemical formation environments.

The water from the spring (MW-04) and the resort well (MW-01) is slightly alkaline (pH 7.7–8.5).

The TDS of the studied waters varies widely, from 0.5 to 12.8 g/L (Table 1). Based on TDS values, the waters are classified as fresh (TDS ~0.5 g/L), brackish (~1.8 g/L), and saline (up to 12.8 g/L). Despite this variation, the hydrochemical type for most samples is chloride-sulfate sodium-calcium (Cl-SO_4-Na-Ca) (Figure 3). The exception is the MW-01 spring, which has a sodium-calcium chloride (Cl-Na-Ca) composition and is associated with Carboniferous limestones.

Chloride (Cl^-) is the dominant anion in all studied waters, constituting 55–94% meq of the total anionic composition. In samples MW-02, MW-03, and MW-04, sulfate ions (SO_4^{2-}) play a significant role, accounting for 25–36% meq. Sodium is the predominant cation (53–70% meq), with a significant calcium content (30–46% meq). Magnesium plays a subordinate role (0.1–0.3% meq). The high Ca^{2+}/Mg^{2+} ratio (>200) in samples MW-01 (360) and MW-04 (223) suggests an evaporitic origin or gypsum dissolution.

Analysis of component distribution versus TDS shows that as TDS decreases (from 12.8 to 0.5 g/L), the proportion of sulfate ions increases from 5% meq in high-TDS water (MW-01) to 36% meq in low-TDS waters (MW-02 to MW-04). This trend indicates mixing between deep, high-TDS waters (Cl-Na-Ca composition) associated with Carboniferous limestones and low-TDS meteoric waters. Furthermore, in all samples with elevated sulfate and low TDS, the sulfate coefficient ($rSO_4 \cdot 100/rCl$) reaches 35–64, which is characteristic of waters formed in zones of active water exchange involving atmospheric precipitation. Thus, the wide TDS range of the Jety-Oguz waters results from the dilution of high-TDS waters with low-TDS waters in varying proportions.

The molar Na/Cl ratio varies from 0.5 to 1.3. In samples MW-01 and MW-04, values are <1 (0.5 and 0.8, respectively), suggesting cation exchange processes where sodium ions are sorbed onto clay minerals, or the precipitation of Na-bearing minerals. In samples MW-02 and MW-03, values are 1.2 and 1.3, respectively, indicating an additional sodium source not solely from halite dissolution (Figure 5). This is likely the result of cation exchange between the water and sodium-rich aluminosilicate rocks, such as sodic plagioclase.

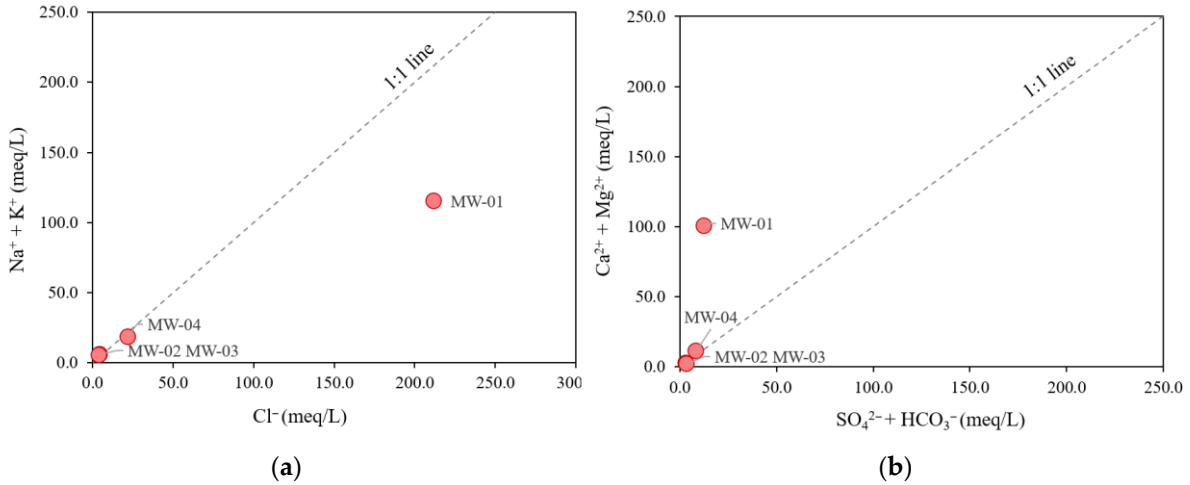


Figure 5. Binary plots of ($Na^+ + K^+$) vs. Cl^- (**a**) and ($Ca^{2+} + Mg^{2+}$) vs. ($SO_4^{2-} + HCO_3^-$) (**b**) for assessing ion exchange and hydrogeochemical processes in the Jety-Oguz mineral waters.

The highest TDS waters (12.8 g/L) are characterized by high chloride (up to 94% meq) and sodium (up to 53% meq) contents, indicating a deep origin and prolonged interaction with host sedimentary rocks. In contrast, low-TDS samples (1.8 and 0.5 g/L) have a mixed composition and are typically associated with the zone of active water exchange. These

waters exhibit elevated bicarbonate (up to 24% meq) and calcium (up to 40% meq) levels, confirming their formation under conditions of active water exchange and partial leaching of the host rocks.

In summary, the waters of the Jety-Oguz area can be divided into two main groups:

- high-TDS thermal mineral waters of sodium-calcium chloride composition, formed within the sedimentary cover of the artesian basin;
- low-TDS waters of mixed chloride-sulfate sodium-calcium composition, formed by the dilution of deep fluids with low-TDS meteoric waters.

The ammonium ion (NH_4^+) concentration in mineral water sample MW-03 is 6.6 mg/L, significantly exceeding both the EU standard (0.5 mg/L) [24] and the WHO guideline value (1.5 mg/L). This may be due to contamination of agricultural origin. In the other mineral water samples (MW-01, MW-02, MW-04), the concentrations of nitrate (NO_3^-), nitrite (NO_2^-), and ammonium (NH_4^+) are within permissible limits.

4.3. Trace Element Composition

The trace element composition of the studied waters varies widely, reflecting the diversity of their hydrogeochemical formation environments (Figure 6). Surface waters (Lake Issyk-Kul, rivers, streams) are characterized by minimal concentrations of most trace elements (Table 2).

The highest concentrations of Sr (43.4 mg/L), Si (23.7 mg/L), B (11.3 mg/L), Li (5.5 mg/L), and Br (1.6 mg/L) were found in the MW-01 mineral water sample (Figure 6), indicating deep-seated fluid alteration and prolonged interaction with the host rocks. In contrast, the lowest concentrations are characteristic of waters from the alluvial horizon (MW-02, MW-03), resulting from circulation under conditions of active water exchange. Samples MW-02, MW-03, and MW-04 show relatively low and similar values for most elements, reflecting comparable formation conditions within the active circulation zone. Their distinct geochemical signature is enriched in some elements (F) and depleted in others (Li, B) compared to MW-01. This contrast highlights a different genesis.

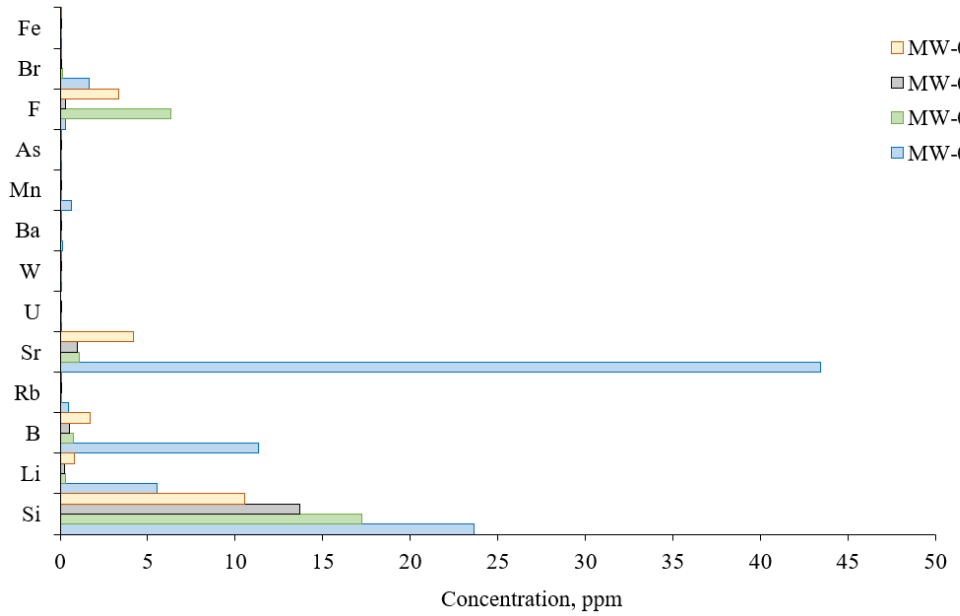
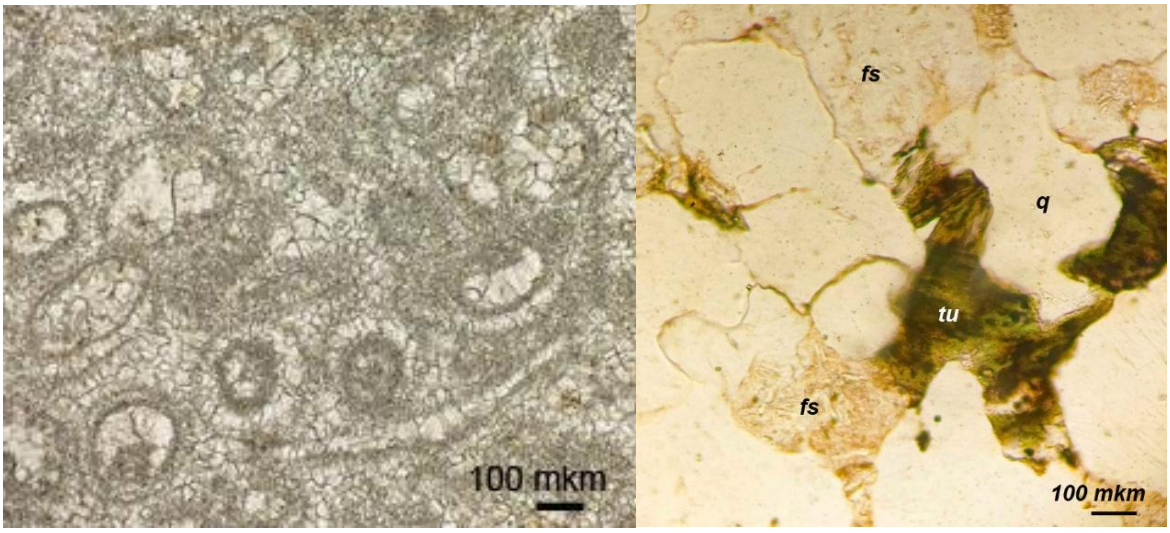


Figure 6. Concentrations of selected trace elements in the mineral waters of the Jety-Oguz area.

Table 2. Trace element concentrations in the studied water samples.

ID	Type of Water Source	Si	Li	B	Rb	Sr	U	W	Ba	Mn	As	F	Br	Fe
		Units (ppb)												
L-01	Lake	5950.7	61.8	1697.9	4.6	4342.8	49.1	6.0	33.1	1.7	12.3	12,300.0	1240.0	210.3
L-02	Lake	5538.4	64.5	1891.9	4.0	4460.0	49.0	6.1	34.6	0.3	13.0	12,600.0	50.0	20.6
L-03	Lake	5070.0	71.1	1443.6	3.9	4857.7	50.0	6.4	40.5	1.0	12.5	300.0	50.0	77.1
R-01	River	2015.5	47.8	89.9	5.2	353.8	2.4	0.5	13.7	0.1	2.0	300.0	50.0	1.4
R-02	River	3951.0	6.2	25.8	2.0	222.3	14.8	0.1	114.4	0.0	1.2	710.0	50.0	0.8
R-03	River	1839.0	3.3	9.8	1.7	72.4	3.5	0.4	12.2	2.7	1.2	460.0	50.0	161.5
R-04	River	1216.0	2.1	9.4	0.7	128.5	8.4	0.1	11.3	0.3	2.0	670.0	50.0	14.0
MW-01	Spring (well)	23,667.3	5539.0	11,329.6	499.1	43,439.9	0.0	41.0	157.2	652.1	65.4	300.0	1640.0	15.9
MW-02	Spring (well)	17,240.7	294.0	754.5	9.7	1068.1	0.3	95.3	20.9	48.3	13.2	6340.0	130.0	54.2
MW-03	Spring (well)	13,710.0	267.7	532.9	8.3	978.2	0.3	89.7	22.5	44.5	12.6	300.0	50.0	66.2
MW-04	Spring	10,532.8	829.9	1691.7	47.0	4186.1	0.0	54.5	26.7	103.0	1.9	3320.0	50.0	15.6

Strontium (Sr) content varies from 0.98 to 43.4 mg/L (Table 2), significantly exceeding the Clarke value for the hydrogenetic zone (0.18 mg/L) and approaching or surpassing that of seawater (8.1 mg/L) [27]. The highest concentration (43.4 mg/L) in the warm (32.0 °C), high-TDS (12.8 g/L) MW-01 water is linked to Carboniferous carbonate deposits. Petrographic studies reveal that 30% of the limestone consists of foraminifera shells (Figure 7a). The high Sr content, despite undersaturation with respect to celestine (SI = −0.52) (Table 3), results from the leaching of strontium from the biogenic limestone's carbonate cement. An additional source may be the dissolution of celestine ($SrSO_4$) from associated evaporite formations. The Sr content in MW-04 (4.19 mg/L) suggests mixing of deep brines with low-TDS waters, while the lowest concentrations in MW-02 and MW-03 are consistent with their low TDS and active water exchange.



(**a**) (**b**)

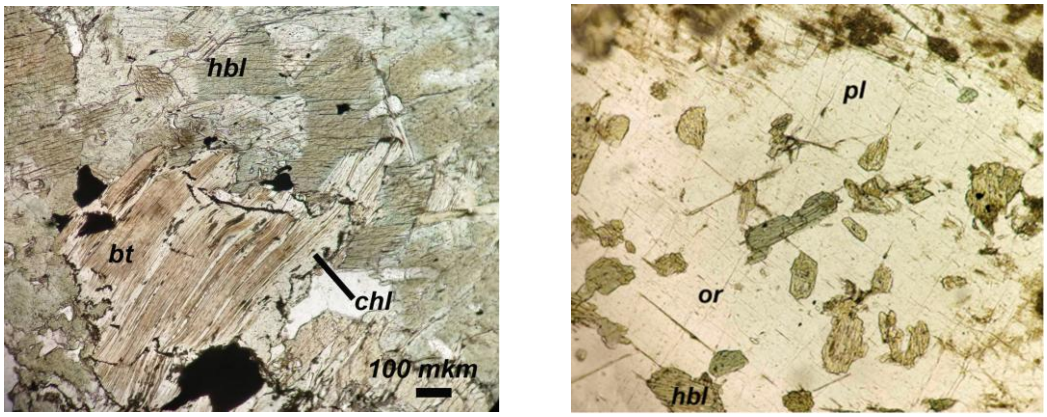
Figure 7. Photomicrographs of thin sections: (**a**) Foraminiferal limestone, plane-polarized light. Shells of foraminifera are visible in a carbonate cement demonstrating a granoblastic texture; (**b**) Tourmaline in aplite (tu), plane-polarized light, associated with quartz (q) and feldspar (fs).

Table 3. Calculated saturation index of minerals in the studied water samples.

ID		MW-01	MW-02	MW-03	MW-04
TDS, g/L		12.8	0.50	0.48	1.83
pH		7.7	9.2	6.5	8.5
T, (°C)		32.0	22.0	22.0	17.9
Eh, mV		−37.5	−134.9	-	−81.2
Mineral	Formula	Saturation index (SI)			
Halite	NaCl	−3.549	−6.280	−6.341	−5.137
Bischofite	$MgCl_2\ 6H_2O$	−10.534	−14.483	−14.618	−13.008
Fluorite	CaF_2	−1.077	0.800	−1.878	0.732
Gypsum	$CaSO_4{\cdot}2H_2O$	−0.570	−1.792	−1.822	−1.007
Anhydrite	$CaSO_4$	−0.674	−1.999	−2.028	−1.254
Celestite	$SrSO_4$	−0.519	−1.790	−1.817	−1.059
Barite	$BaSO_4$	0.234	−0.168	−0.129	0.125
Mirabilite	$Na_2SO_4{\cdot}10H_2O$	−4.538	−6.456	−6.538	−5.060
Epsomite	$MgSO_4\ 7H_2O$	−5.695	−6.387	−6.481	−5.904
Calcite	$CaCO_3$	0.720	0.837	−1.843	0.793
Dolomite	$CaMg(CO_3)_2$	−0.033	0.584	−4.841	0.147
Aragonite	$CaCO_3$	0.557	0.672	−2.008	0.627
Magnesite	$MgCO_3$	−2.342	−1.901	−4.646	−2.319
Witherite	$BaCO_3$	0.663	1.681	−0.931	1.175
Strontianite	$SrCO_3$	1.484	1.686	−0.991	1.642
Quartz	SiO_2	0.839	0.759	0.753	0.690
Chalcedony	SiO_2	0.574	0.485	0.479	0.413
Kaolinite	$Al_2(Si_2O_5)(OH)_4$	1.900	−0.373	3.430	2.570
Illite	$K_{0,65}Al_{2,0}(Al_{0,65}Si_{3,35}O_{10})(OH)_2$	2.838	0.580	1.994	3.352
Muscovite	$KAl_2(AlSi_3O_{10})(F,OH)_2$	4.139	0.877	3.908	4.973
Anorthite	$Ca(Al_2Si_2O_8)$	−3.640	−5.129	−6.656	−3.315
Albite	$Na(AlSi_3O_8)$	2.035	0.726	−0.076	1.790
Talc	$Mg_3Si_4O_{10}(OH)_2$	0.124	4.482	−11.725	0.264
Epidote	$Ca_2Al_2Fe_3(SiO_4)_3OH$	5.964	6.468	−0.464	6.989
Hematite	Fe_2O_3	10.468	11.875	11.735	11.194
Goethite	FeO(OH)	4.742	5.464	5.394	5.130
Uraninite	UO_2	−22.776	−17.542	4.312	−23.671

Silicon (Si) concentrations range from 10.5 to 23.7 mg/L (Table 2), exceeding Clarke values for both the hydrogenetic zone (8.4 mg/L) and seawater (2.1 mg/L) [27]. The highest value (23.7 mg/L) was found in the deep well MW-01. Elevated levels were also recorded in sample MW-04 (17.9 mg/L), collected from a spring at a temperature of 17.9 °C. The lowest silicon concentrations were found in the waters of the alluvial horizon: 13.7 mg/L (MW-03) and 17.2 mg/L (MW-02) at a temperature of 22.0 °C.

The content of metasilicic acid (H_2SiO_3) in all studied waters (17.7–30.6 mg/L) falls short of the 50 mg/L threshold for siliceous waters, thus classifying them as slightly siliceous. A positive correlation exists between silicon content and water temperature (R^2 = 0.9). Petrographic studies identify widely distributed quartz, feldspar, and biotite as the source of silicon, with dissolution intensifying at elevated temperatures (Figure 8).



(**a**) (**b**)

Figure 8. Photomicrographs of thin sections: (**a**) Biotite-hornblende association. Biotite is crenulated and replaced by chlorite, plane-polarized light; (**b**) Monzonitic texture of monzodiorite. Poikilitic inclusions of hornblende (hbl) and plagioclase (pl) within an allotriomorphic grain of potassium-sodium feldspar (or), plane-polarized light.

Lithium (Li) concentrations (0.27–5.54 mg/L) far exceed Clarke values for the hydrogenetic zone (0.013 mg/L) and seawater (0.170 mg/L) [27]. The primary source is the leaching of aluminosilicate minerals (e.g., micas, clays) during prolonged water–rock interaction in the deep parts of the basin [28]. The low Li content in MW-02 and MW-03 confirms their classification as active water exchange waters in alluvial deposits.

Boron (B) shows a wide range (0.53–11.33 mg/L) (Table 2), an order of magnitude above the hydrogenetic zone Clarke value (0.08 mg/L) and more than double that of seawater (4.5 mg/L) [27]. A strong positive correlation with TDS ($R^2 = 0.99$) exists. The high concentration in MW-01 (11.33 mg/L) indicates a connection to ancient sedimentary brines. On the other hand, the petrographically confirmed presence of tourmaline in aplites (Figure 7b) and the processes of biotite chloritization in monzodiorites indicate that boron and lithium were introduced through the interaction of deep fluids with the basement rocks (Figure 8). The intermediate value in MW-04 (1.69 mg/L) suggests mixing, while low values in MW-02 and MW-03 confirm the absence of a deep boron source.

Bromine (Br) concentrations (0.05–1.64 mg/L) (Table 2) significantly exceed respective Clarke values [27]. The high Br content in MW-01, combined with a Cl/Br ratio of 4584, points to dissolution of halite and concentration of residual brines [28]. Low Br in other samples is characteristic of infiltration waters.

Fluorine (F) content varies from 0.3 to 6.34 mg/L, exceeding Clarke values [27]. The highest concentration was found in MW-02, with elevated levels also in MW-04 (Table 2). The source is the hydrolysis of F-bearing aluminosilicate minerals (e.g., biotite, hornblende) in the bedrock. Petrographic studies of the monzodiorites (Figure 8b) confirm the presence of biotite and hornblende in the bedrock. An important factor contributing to fluoride accumulation is the slightly alkaline environment (pH = 8.5–9.2) and relatively low calcium content in these waters, which inhibits the formation of poorly soluble fluorite. The lowest F concentration was found in the high-TDS sample MW-01.

The saturation indices (Table 3) for sample MW-01 show oversaturation with respect to calcite (SI = 0.72) and aragonite (SI = 0.56) (Figure 9), consistent with its slightly alkaline pH (7.7) and equilibrium with the carbonate reservoir. At the same time, the water is undersaturated with respect to halite (SI = −3.55), bischofite (SI = −10.53), gypsum (SI = −0.57), anhydrite (SI = −0.67), and celestine (SI = −0.52) (Figure 9). This indicates ongoing dissolution of these minerals and a continuous influx of sodium, chloride, sulfate, and strontium ions into the solution.

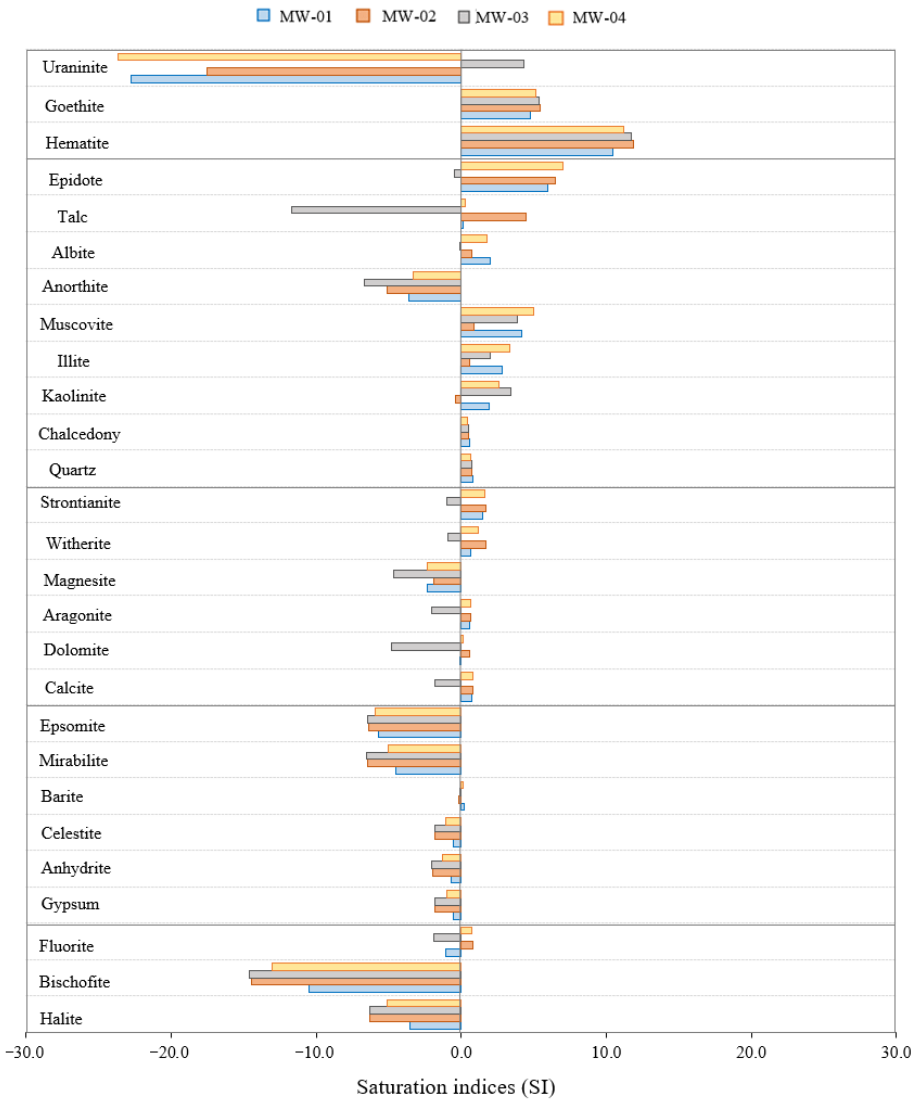


Figure 9. Mineral saturation indices (SI) for the Jety-Oguz mineral waters.

The chemical composition of a secondary phase (Tables 4 and 5), sampled at the discharge point of the high-TDS thermal water (sample MW-01), is characterized by a high Na_2O content (41.48%), significant loss on ignition (LOI = 49.08%), and a low sulfur concentration (1.13%).

Table 4. Chemical composition of water-bearing rocks and secondary phase from the Jety-Oguz area.

Sample ID	Rock Type	SiO_2	TiO_2	Al_2O_3	Fe_2O_3	MnO	MgO	CaO	Na_2O	K_2O	P_2O_5	H_2O^-	LOI	Total
		wt. %												
1	Limestone	5.69	0.01	0.07	0.15	0.22	0.13	50.44	0.03	0.02	0.01	0.08	39.27	96.12
2	Monzodiorite	50.76	1.32	15.63	10.01	0.16	6.27	6.11	2.31	3.68	0.54	0.31	2.70	99.79
3	Aplite	73.44	0.16	12.36	1.73	0.03	0.55	1.38	2.66	5.12	0.05	0.24	2.08	99.79
4	Siltstone	63.70	0.42	11.28	2.02	0.06	4.28	5.61	2.36	2.35	0.15	0.99	6.50	99.72
5	Secondary phase	0.81	0.01	0.02	0.07	0.00	0.01	2.50	41.48	0.03	0.01	4.03	49.08	98.06

Table 5. Trace element composition of water-bearing rocks and secondary phase from the Jety-Oguz area.

Sample ID	1	2	3	4	5
Rock Type	Limestone	Monzodiorite	Aplite	Siltstone	Secondary Phase
			Units (ppm)		
Li	3.579	20.59	6.583	65.18	14.49
Be	0.014	1.801	1.158	1.283	0.011
S	9312	<1000	<1000	<1000	11,315
Sc	0.367	21.45	5.271	13.21	0.059
V	0.897	157.5	25.16	88.34	0.133
Cr	0.976	241.1	10.90	26.34	0.594
Co	1.039	33.00	3.757	9.013	0.072
Ni	0.808	77.27	5.558	13.41	0.194
Cu	6.631	25.80	4.443	21.74	0.738
Zn	5.112	112.6	20.14	76.52	1.014
Ga	0.122	17.19	10.63	11.99	0.033
Ge	0.126	1.618	1.156	1.771	0.117
As	1.915	3.185	2.517	8.139	5.713
Se	0.026	0.200	0.126	0.111	0.002
Rb	0.674	166.2	190.9	78.41	1.600
Sr	1368	351.6	150.7	146.6	183.7
Y	4.690	32.51	11.12	17.34	0.116
Zr	1.595	7.458	53.03	94.65	0.765
Nb	0.088	17.13	5.340	7.119	0.036
Mo	0.068	0.255	0.144	0.189	0.207
Ag	0.005	0.009	0.030	0.052	0.002
Cd	0.081	0.095	0.080	0.104	0.027
Sn	0.119	1.981	1.699	1.627	0.129
Sb	0.032	0.108	0.716	0.553	0.061
Te	0.007	0.009	0.009	0.038	0.003
Cs	0.077	1.214	3.232	7.678	0.529
Ba	33,157	1897	1328	467.8	3.084
Hf	0.053	0.529	1.899	2.875	0.056
Ta	0.011	0.753	0.440	0.473	0.004
W	4.213	1.910	0.811	1.383	1.780
Tl	0.012	0.666	0.923	0.357	0.019
Pb	1.221	7.221	15.69	5.024	0.965
Bi	0.171	0.047	0.222	0.241	0.003
Th	0.101	3.486	10.56	7.927	0.019
U	0.285	0.752	1.437	2.842	0.017

The ratio of these components indicates that the secondary phase consists predominantly of highly soluble sodium chloride (halite) with minor sulfate impurities. The low concentrations of SiO_2 (0.81%) and Al_2O_3 (0.02%) rule out any substantial contribution from silicate or clay minerals. Thus, the composition of this secondary phase results from salt crystallization triggered by abrupt changes in the physicochemical conditions of the discharging MW-01 mineral water and subsequent evaporative concentration, which is fully consistent with its Cl-Na-Ca hydrogeochemical type.

The trace element composition of the secondary phase shows elevated contents of lithium (14.5 mg/kg), strontium (183.7 mg/kg), and arsenic (5.7 mg/kg). This serves as an indicator of concentration processes affecting the high-TDS mineral waters in their discharge zone and confirms the supply of these elements by deep fluids (Table 5).

https://doi.org/10.3390/w18010075

4.4. Total Carbon Content

The total carbon (TC) content in the studied mineral water samples indicates a significant predominance of the inorganic fraction (Figure 4). The mineral waters exhibit minimal TOC values (0.1–0.8 mg/L), with samples MW-02 and MW-03 showing higher Inorganic Carbon (IC) content than MW-01 and MW-04.

4.5. Gas Composition

In terms of gas composition, the Jety-Oguz mineral waters are of the nitrogen type, with free nitrogen content ranging from 97 to 100 vol.%. Minor amounts of carbon dioxide, methane, and trace noble gases are also present.

4.6. Isotopic Composition

The isotopic composition of the studied waters varies widely, with $\delta^{18}O$ values ranging from −13.4‰ to 0.5‰ and δD values from −91.5‰ to −2.6‰ (Figure 10, Table 6).

Table 6. Stable isotope composition of natural waters and precipitation.

ID	Type of Water Source	Elevation	$\delta^{18}O$	$\delta^{2}D$
		m a.s.l.	‰	
P-01	Rain	2031.0	0.5	−2.6
L-01	Lake	1601.0	−1.0	−15.2
L-02	Lake	1601.0	−0.3	−12.5
L-03	Lake	1567.0	0.5	−9.4
R-01	River	2128.0	−11.6	−73.0
R-02	River	2132.0	−10.4	−75.5
R-03	River	2038.0	−5.0	−55.1
R-04	River	2298.0	−5.9	−58.3
MW-01	Spring (well)	2042.0	−10.8	−77.8
MW-02	Spring (well)	2195.0	−13.4	−89.4
MW-03	Spring (well)	2127.0	−13.0	−90.5
MW-04	Spring	2126.0	−13.4	−91.5

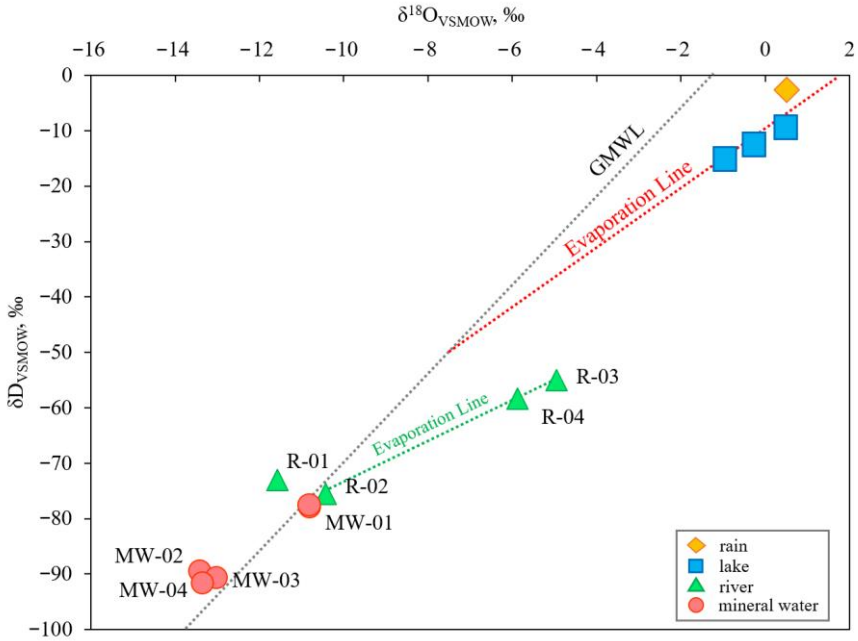


Figure 10. Stable isotope plot (δD_{VSMOW} vs. $\delta^{18}O_{VSMOW}$) of natural waters from the Jety-Oguz area relative to the Global Meteoric Water Line (GMWL).

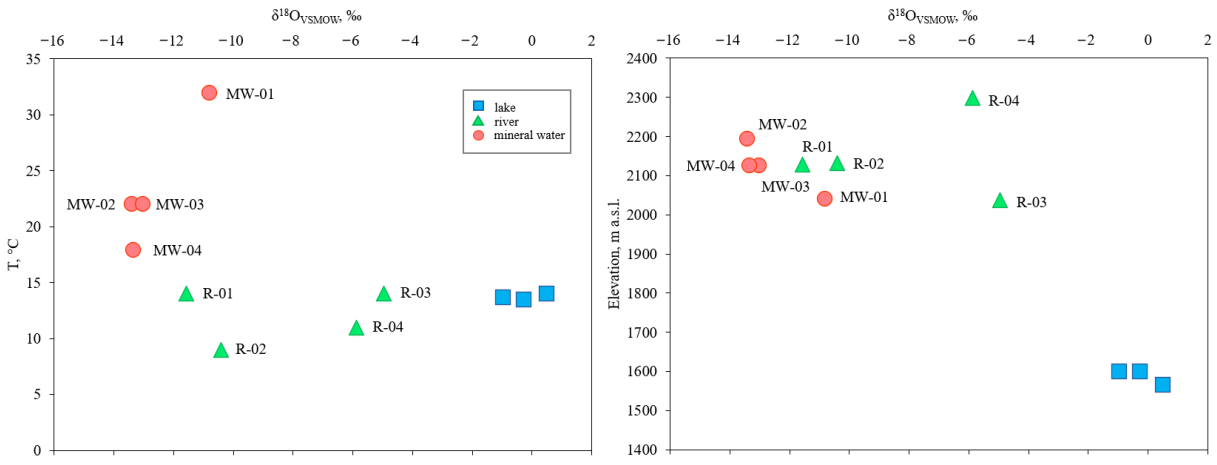
The waters of Lake Issyk-Kul (L-01, L-02, L-03) plot along a local evaporation line, which is characteristic of surface waters in this endorheic basin. The precipitation sample (P-01), collected during the warm summer period (June), exhibits the highest isotopic values ($\delta^{18}O$ = 0.5‰, δD = −2.6‰), consistent with seasonal effects.

River waters (R-01, R-02, R-03, R-04) are characterized by a relatively light isotopic composition. Samples R-01 and R-02 ($\delta^{18}O$ from −11.6‰ to −10.4‰; δD from −75.5‰ to −73.0‰) plot near the Global Meteoric Water Line, or GMWL [8], confirming their meteoric origin. In contrast, waters from R-03 and R-04 are significantly enriched in heavy isotopes ($\delta^{18}O$ up to −5.0‰, δD up to −55.1‰). Their position to the right of the GMWL indicates the influence of evaporative fractionation, a common process in the middle and lower river reaches where slower flow and high air temperatures intensify evaporation. Despite this enrichment, the TDS of these waters remains low (0.1–0.2 g/L) due to seasonal dilution by meltwater and precipitation.

Based on isotopic data, the mineral waters can be divided into two genetic groups. The first group (MW-02, MW-03, MW-04) has a light isotopic composition ($\delta^{18}O$ from −13.4‰ to −13.0‰; δD from −91.5‰ to −89.4‰), indicating a high-altitude (primarily snowmelt) recharge source. The second group is represented solely by the MW-01 spring ($\delta^{18}O$ = −10.8‰, δD = −77.8‰), which is associated with fractured Carboniferous limestones. Despite its high TDS (12.8 g/L) and elevated temperature (32 °C), MW-01 plots on the GMWL, confirming its meteoric origin. This apparent paradox can be explained by its rapid circulation through fracture-vein systems and quick discharge along tectonic faults, which minimizes evaporation and isotopic fractionation. Furthermore, the temperature appears insufficient to drive significant oxygen isotope exchange with the host rocks.

Thus, the high-TDS water of MW-01 represents infiltrating meteoric water that has been geochemically transformed but has preserved its isotopic signature in a relatively closed hydrogeochemical system.

For all studied waters, there is no pronounced correlation between $\delta^{18}O$ and temperature (Figure 11). The observed weak negative correlation can be explained by the fact that the warmer waters (mineral springs) are recharged at high altitudes, which imparts a lighter isotopic composition. Consequently, the water temperature in this context is not the cause of the isotopic variation but rather reflects the circulation patterns: high-altitude recharge sources have deeper circulation paths and, as a result, higher temperatures upon discharge.



(**a**) (**b**)

Figure 11. Relationships between $\delta^{18}O_{VSMOW}$ values and water temperature (**a**), and between $\delta^{18}O_{VSMOW}$ values and absolute elevation (**b**) for natural waters in the Jety-Oguz area.

In summary, the mineral waters of the Jety-Oguz area are predominantly of meteoric origin, as unequivocally demonstrated by their stable isotope composition.

4.7. Geothermometry and Circulation Depth

To estimate the reservoir temperatures of the mineral waters, we applied a suite of cation geothermometers [11,14–17].

The calculated temperatures show a wide range, from 30.8 to 160.2 °C (Table 7, Figure 12), reflecting differences in circulation depth and genesis.

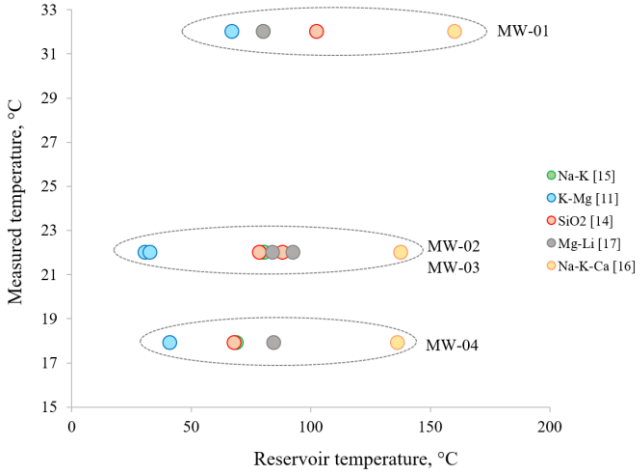


Figure 12. Comparison of measured temperatures and reservoir temperatures estimated by different chemical geothermometers for the Jety-Oguz mineral waters.

Table 7. Calculated reservoir temperatures from chemical geothermometers for the studied waters.

ID	Type of Water Source	*T* (°C)	Reservoir Temperature (°C)				
			Na-K [15]	K-Mg [11]	SiO_2 [14]	Mg-Li [17]	Na-K-Ca [16]
MW-01	Spring (well)	32.0	80.2	67.0	102.4	80.3	160.2
MW-02	Spring (well)	22.0	80.1	30.8	88.2	92.7	137.8
MW-03	Spring (well)	22.0	80.6	32.7	78.5	84.2	137.6
MW-04	Spring	17.9	68.9	41.0	68.1	84.6	136.3

The Na-K geothermometer [15] yielded temperatures from 68.9 to 80.6 °C but is considered less reliable for waters from the active water exchange zone. The K-Mg geothermometer [11] provided more plausible estimates: 67 °C for sample MW-01 and 30.8–32.7 °C for the active water exchange waters (MW-02, MW-03), the latter being close to their measured discharge temperatures. The most reliable estimate for the deep fluid (MW-01) was obtained using the quartz geothermometer [14], indicating a formation temperature of 102.4 °C. Sample MW-04 shows an intermediate quartz temperature of 68.1 °C, supporting a formation model involving mixing between the ascending thermal water (MW-01 type) and cold, low-TDS waters (MW-02, MW-03 type).

The genetic classification of the waters is further validated by the Giggenbach Na-K-Mg ternary diagram [11]. The thermomineral water sample (MW-01) plots near the full equilibrium zone, indicating prolonged water–rock interaction at elevated temperatures and confirming the reliability of the cation geothermometer results for this sample (Figure 13). In contrast, the MW-02 and MW-03 samples plot within the immature water field, typical for waters evolving under active water exchange conditions; this explains the inconsistent and often overestimated temperatures derived from cation geothermometers for these samples. The position of the MW-04 sample in the partial equilibrium region reflects the mixing of deep, high-TDS thermal water with shallow alluvial waters.

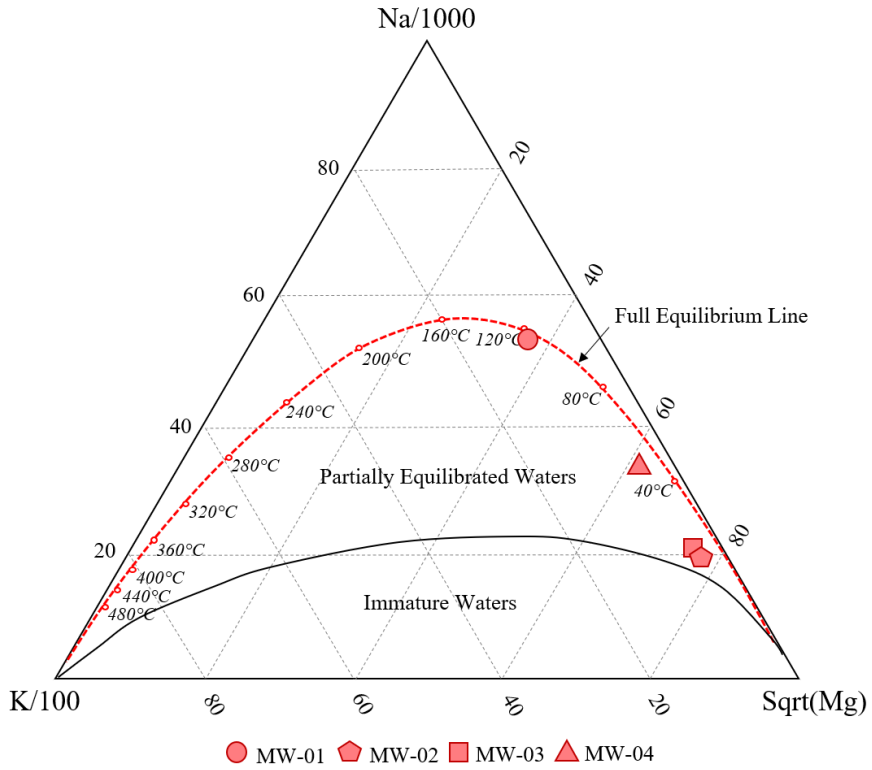


Figure 13. Giggenbach diagram for the assessment of reservoir temperature and equilibrium state of the Jety-Oguz mineral waters.

In summary, the integrated application of geothermometers establishes that the thermomineral waters (MW-01) are formed at temperatures of approximately 105 °C, whereas the active water exchange zone waters (MW-02, MW-03) are characterized by near-surface temperatures of about 30 °C.

The circulation depth (H, km) of the studied waters was calculated using a standard method based on the geothermal gradient and the formula

$$H = (T_{reservoir} - T_{surface})/K + z_0, \quad (1)$$

where $T_{reservoir}$ is the temperature obtained from the geothermometer (°C); $T_{surface}$ is the mean annual air temperature (°C); K is the geothermal gradient (°C/km); and z_0 is the depth of the neutral layer (km).

For the high-altitude Jety-Oguz area (2050 m a.s.l.), the following parameters were adopted: mean annual air temperature 6 °C; geothermal gradient 32 °C/km; neutral layer depth 0.022 km [19,20].

The calculations indicate that the high-TDS thermal waters (MW-01) form at depths of approximately 3.0 km. Mixed waters (MW-04) circulate at depths up to 2.0 km, while the low-TDS alluvial waters (MW-02, MW-03) in the active water exchange zone form at depths of up to 0.8 km.

4.8. Hydrogeochemical Formation Processes

The Gibbs diagram was used to identify the dominant processes controlling the chemical composition of the mineral waters, in line with the established circulation depths. The position of the studied surface (Lake Issyk-Kul, rivers) and groundwater (mineral springs) samples on the diagram (Figure 14) reveals several genetic groups and clearly illustrates the diversity of hydrogeochemical conditions in the region.

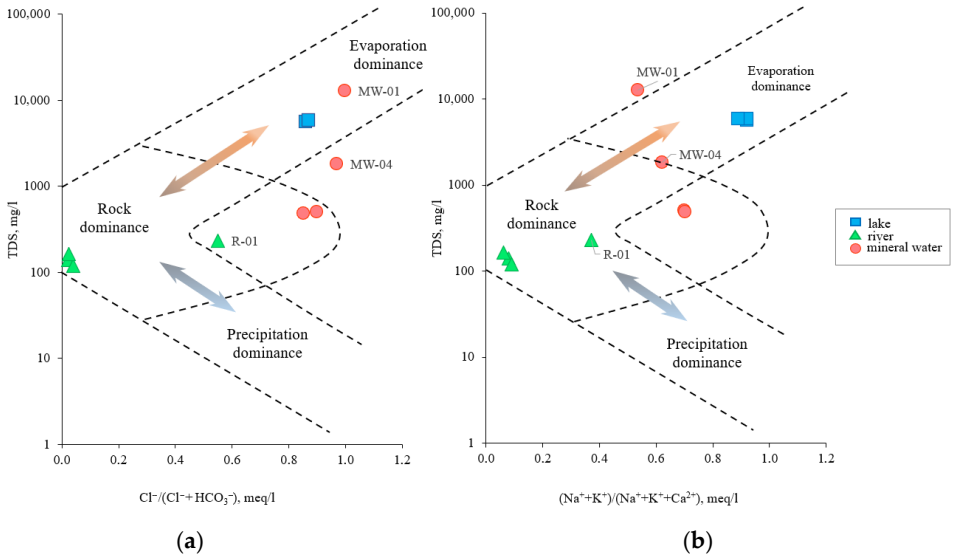


Figure 14. Gibbs diagrams for (**a**) anions and (**b**) cations, showing the dominant processes controlling the chemical composition of Jety-Oguz mineral waters.

Water samples from Lake Issyk-Kul (L-01, L-02, L-03) plot on the right side of the Gibbs diagram within the zone where evaporation is the dominant process. This naturally leads to high TDS (5.6–5.9 g/L), a characteristic feature of endorheic basins.

The mineral water sample MW-01 also falls within the evaporation dominance zone, but this is due to a different mechanism. In a closed hydrogeological system at elevated temperatures, intensive dissolution of highly soluble minerals (e.g., halite, gypsum) occurs, leading to high TDS (12.8 g/L) and enrichment in sodium and chloride ions. Thus, the Gibbs diagram here reflects a process of deep-seated salt concentration that is geochemically analogous to evaporation.

In contrast, the MW-02 and MW-03 mineral waters, circulating in shallow alluvial deposits, plot within the rock dominance zone. Their composition is formed under conditions of active water exchange, where infiltrating meteoric water rapidly interacts with aluminosilicate and carbonate minerals of the alluvium, resulting in low TDS (0.5 g/L) and a distinct hydrochemical facies.

The MW-04 mineral water sample occupies an intermediate position between the MW-01 and MW-02/MW-03 samples on the Gibbs diagram, indicating a mixing process between these two genetically different water types.

To quantify the mixing proportion in sample MW-04, a binary mixing model was applied using conservative tracers – chloride (Cl^-), total dissolved solids (TDS), and the isotopic composition ($\delta^{18}O$), in accordance with standard methodology [18]:

$$f_A = \frac{Cmix - CB}{CA - CB}, \quad (2)$$

where C*mix* is the tracer concentration in the MW-04 sample, mg/L; C*A* is the tracer concentration in the MW-01 sample, mg/L; C*B* is the tracer concentration in the MW-02 and MW-03 samples, mg/L.

The calculation based on chloride concentration shows that the MW-04 sample consists of 8.5% deep high-TDS fluid (MW-01) and 91.5% water from the active water exchange zone (Figure 15). The calculation using TDS yields a similar result, indicating approximately 10.6% deep fluid and 89.4% active water exchange water. The isotopic data provide further insight (Figure 16). Samples MW-02 and MW-04 have an identical isotopic composition ($\delta^{18}O$ = −13.4‰), indicating a common high-altitude (snowmelt) recharge source. The absence of a discernible influence from the heavier isotopic signature of the

MW-01 fluid ($\delta^{18}O = -10.8‰$) is explained by its small mixing fraction. This demonstrates that while the chemical composition of MW-04 was altered by the addition of the deep fluid, its isotopic composition remained unchanged, being dominated by the meteoric end-member.

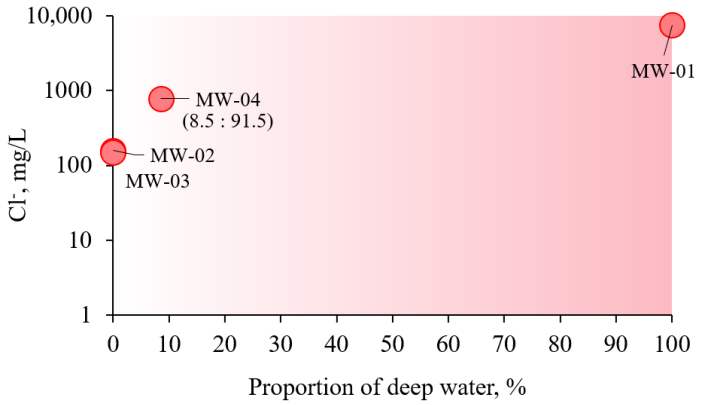


Figure 15. Estimated proportions of deep component in the Jety-Oguz water samples.

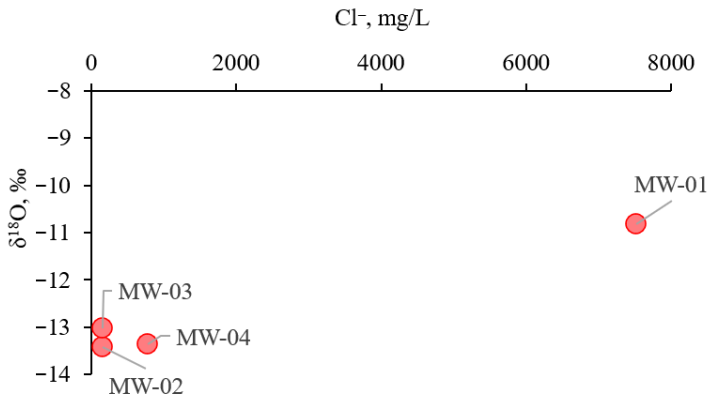


Figure 16. Relationship between $\delta^{18}O$ values and chloride concentration in Jety-Oguz mineral waters.

Therefore, we conclude that the MW-04 sample is predominantly water formed in the zone of active water exchange from atmospheric precipitation, with a minor but geochemically significant contribution from a deep fluid.

4.9. Element Mobility Assessment

To quantify the migration ability of chemical elements in the water–rock system of the Jety-Oguz area, we applied the aqueous migration coefficient (Kx) proposed by A.I. Perelman [21]. This coefficient assesses an element's propensity to pass into solution relative to its average crustal abundance (clarke) and is calculated using the formula

$$Kx = \frac{100 m_x}{M n_x}, \quad (3)$$

where m_x is the element content in water (mg/L); M is the TDS of water (mg/L); and n_x is the element content in the host rock or its clarke value (mg/kg).

Grouping elements by their Kx values helps build a geochemical model and identify elements that are actively leached from rocks and concentrated in the water. A higher Kx value indicates more intense migration and a greater capacity for removal from the host sediments.

The intensity of elemental migration is influenced by a complex of factors, including the element's initial concentration in the rock (clarke), its inherent geochemical properties, hydrodynamic conditions, TDS and temperature [27,29–31].

To assess component mobility in the Jety-Oguz mineral waters, the Kx was calculated for macro- and microcomponents relative to their concentrations in the area's main rock types (limestone, siltstone, aplite, monzodiorite) and relative to their lithospheric clarke values.

Data analysis reveals that elemental migration ability varies significantly depending on the lithology of the host rocks and the hydrogeological conditions. For the high-TDS waters associated with limestones (MW-01), strong migration (Kx > 1) is characteristic of Li, Cl, Na, and Ca. The high Kx of lithium, despite its low clarke in limestones, confirms an external source for this element, likely from the basement rocks. The moderate mobility of strontium, despite its high absolute concentration in the water (43.4 mg/L), is explained by its high concentration in the limestone itself (1368 mg/kg), consistent with a biogenic source.

For the active water exchange zone waters (MW-02, MW-03), strong migration is typical for S, Cl, Sr, and Na. The highest Kx values are observed for sulfur and strontium, indicating active leaching of these elements from the metamorphic and igneous rocks.

Across almost all conditions, chlorine, sodium, and calcium are the strongest migrants (Kx > 10), while potassium consistently shows the lowest migration intensity (Kx < 0.2).

5. Discussion

Comprehensive research on the Jety-Oguz mineral waters has enabled the establishment of their formation conditions and the identification of three distinct genetic types (Figure 17).

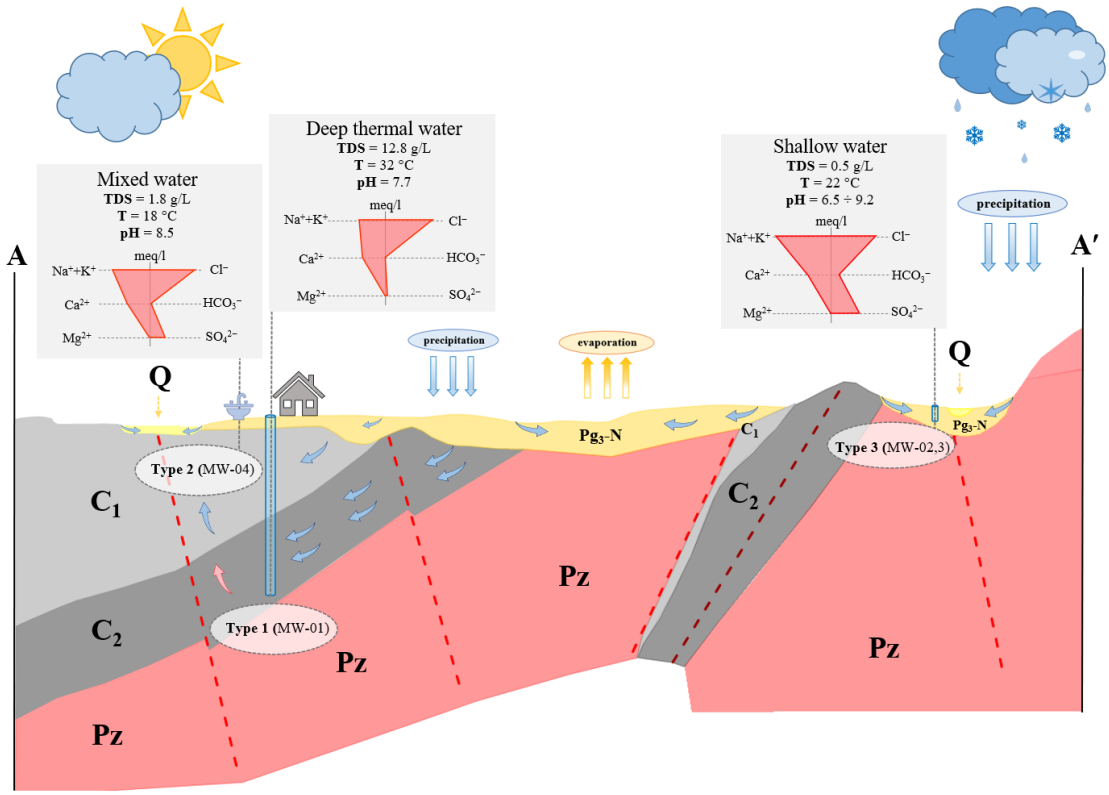


Figure 17. Conceptual scheme of the formation and circulation of mineral waters in the Jety-Oguz area.

https://doi.org/10.3390/w18010075

Type 1: Deep thermal waters (MW-01).

This type is characterized by a sodium-calcium chloride composition, unique for the Issyk-Kul basin, with a TDS of 12.8 g/L (saline water) and a discharge temperature of 32.0 °C. These waters circulate within Middle Carboniferous carbonate deposits at depths of ~3.0 km, with a estimated reservoir temperature of 105 °C based on quartz geothermometry. Their composition results from a combination of processes: meteoric waters of infiltration origin descend through fault zones, where they are heated and interact with rocks of the sedimentary cover. The undersaturation with respect to halite (SI = −3.55) and gypsum (SI = −0.57), despite high corresponding ion concentrations, indicates ongoing dissolution of highly soluble minerals from evaporite formations in the deep subsurface. High strontium concentrations (43.4 mg/L) are linked to the leaching of biogenic limestones, which are 30% composed of foraminifera shells; this explains the water's undersaturation with respect to celestine (SI = −0.52) during active removal of this element. Elevated lithium (5.54 mg/L) and boron (11.33 mg/L) levels are associated with interaction with aluminosilicate basement rocks containing biotite and tourmaline. These waters are of significant balneological value.

Type 2: Mixed waters (MW-04).

This type is formed by the dilution of deep-seated brines with active water exchange waters, occupying an intermediate position with a TDS of 1.8 g/L (brackish water) and a temperature of 17.9 °C. Binary mixing calculations using chloride indicate that these waters contain approximately 10% of the deep fluid and 90% of active water exchange waters. This is corroborated by a shift in the hydrochemical facies from chloride to chloride-sulfate and intermediate trace element concentrations (Li = 0.83 mg/L; Sr = 4.19 mg/L). The stable isotope composition ($\delta^{18}O$ = −13.4‰, δD = −91.5‰) corresponds to a high-altitude snowmelt recharge source, confirming the dominance of the meteoric end-member. These waters have potential for therapeutic and drinking purposes.

Type 3: Shallow groundwaters (MW-02, MW-03).

These waters form in alluvial deposits at depths of up to 0.8 km and are characterized by low TDS (0.5 g/L) (fresh water), a chloride-sulfate composition, and a temperature of 22.0 °C. Their primary recharge source is the infiltration of atmospheric precipitation and snowmelt. The low concentrations of trace elements (Li = 0.27–0.29 mg/L; Sr = 0.98–1.07 mg/L) confirm their formation under conditions of active water exchange. This water type is suitable for domestic drinking water supply, agricultural needs, and fishery purposes.

6. Conclusions

Based on new data from a comprehensive study of the chemical and isotopic composition of the Jety-Oguz mineral waters, we have established the key processes for their formation. The main conclusions are as follows:

1. The Jety-Oguz brachyanticline plays a pivotal role in the hydrogeology of the area. In its near-surface part, deeply incised by the Jety-Oguz river, Paleozoic rocks are exposed, creating a primary discharge zone for deep fluids. Intense fracturing within the Carboniferous limestones in this zone ensures high hydraulic conductivity, facilitating the ascent of deep-seated waters.
2. Three distinct genetic water types have been identified: (1) deep-circulating thermal waters; (2) mixed waters formed by dilution of the deep fluid; and (3) shallow active-exchange waters with low salinity formed in alluvial deposits.
3. The diversity of water compositions arises from a combination of processes: the upward flow of deep brines, their mixing with meteoric waters in varying proportions,

and subsequent hydrogeochemical reactions (including dissolution of halite and gypsum, cation exchange, and leaching of silicate minerals).
4. Stable isotope data ($\delta^{18}O$, δD) confirm a meteoric origin for all water types.
5. The established genetic model has direct practical implications. Type 1 waters are valuable for balneology; Type 2 have potential as therapeutic drinking waters; and Type 3 are suitable for domestic and agricultural supply.

Author Contributions: Conceptualization, investigation, writing—original draft preparation and visualization, project administration, funding acquisition, E.I.B.; writing—review and editing, validation, investigation, N.A.K.; formal analysis, I.A.T., validation, F.S.S.; validation, investigation, G.A.C. All authors have read and agreed to the published version of the manuscript.

Funding: This study was supported by the Russian Science Foundation (RSF), project No. 25-27-00122 "Sources and formation conditions of the salt component in mineral waters of intermountain artesian basins".

Data Availability Statement: The original contributions presented in this study are included in the article. Further inquiries can be directed to the corresponding author.

Acknowledgments: The authors gratefully acknowledge the editors and anonymous reviewers for their valuable comments and constructive suggestions, which significantly improved the quality of this manuscript. We also extend our thanks to our colleagues for their assistance with the chemical and isotopic analyses.

Conflicts of Interest: The authors declare no conflicts of interest.

References

1. Baranovskaya, E.I.; Kharitonova, N.A.; Chelnokov, G.A.; Ermakov, A.V. Isotopic-Hydrogeochemical Characteristics of Thermal Mineral Waters of the Issyk-Kul Artesian Basin. *Mosc. Univ. Geol. Bull*. **2024**, *63*, 142–156. https://doi.org/10.55959/MSU0579-9406-4-2024-63-5-142-156. (In Russian)
2. Kharitonova, N.A.; Sokolovskaya, M.A.; Baranovskaya, E.I.; Chelnokov, G.A.; Karabtsov, A.A.; Chernoshchekov, L.N.; Bragin, I.V. Trace Elements in Thermal Waters of the Northern Tien Shan: Distribution and Accumulation Mechanisms. *Mosc. Univ. Geol. Bull*. **2024**, *63*, 70–86. https://doi.org/10.55959/MSU0579-9406-4-2024-63-4-70-86. (In Russian)
3. Kataeva, N.I.; Melnikova, Z.I.; Barsutskaya, R.D. *Mineral Waters of the Kirghiz SSR*; Ministry of Health of the Kirghiz SSR, Research Institute of Balneology and Physiotherapy: Frunze, Kyrgyzstan, 1969; 142p. (In Russian)
4. Vasilyeva, V.N. Features of the Formation of Jety-Oguz Radioactive Thermal Waters. In Issues of Formation and Distribution of Mineral Waters of the USSR: Proceedings of the Meeting of Resort Institutes on Hydrogeology of Mineral Waters; Ivanov, V.V., Ed.; Central Research Institute of Balneology and Physiotherapy: Moscow, Russia, 1960. (In Russian)
5. Mandychev, A.N. Groundwaters of the Issyk-Kul Basin. In *Lake Issyk-Kul: Its Natural Environment*; Klerkx, J., Imanackunov, B., Eds.; NATO Science Series: IV: Earth and Environmental Sciences; Springer: Dordrecht, The Netherlands, 2002; Volume 13, pp. 71–76.
6. Mandychev, A.N. Resources of Deep Groundwaters of the East-Chuy and Issyk-Kul Artesian Basins. In *High-Mountain Research: Changes and Prospects in the 21st Century*; National Academy of Sciences of the Kyrgyz Republic, Bishkek, Kyrgyzstan, 1996; pp. 136–137. (In Russian)
7. Matychenkov, V.E.; Imanakunov, B.I. *Mineral Waters of Kirghizia*; Ilim: Frunze, Kyrgyzstan, 1987; 251p. (In Russian)
8. Craig, H. Standard for reporting concentration of deuterium and oxygen—18 in natural waters. *Science* **1961**, *133*, 1833–1834.
9. Bethke, C.M. *Geochemical and Biogeochemical Reaction Modeling*, 3rd ed.; Cambridge University Press: New York, NY, USA, 2022.
10. Shestakova, A.V.; Guseva, N.V. Application of Geothermometers for Estimating Deep Circulation Temperatures of Thermal Waters on the Example of Eastern Tuva. *Izv. Tomsk. Polytech. Univ. Eng. Georesour*. **2018**, *329*, 25–36. (In Russian)
11. Giggenbach, W.F. Geothermal Solute Equilibria. Derivation of Na-K-Mg-Ca Geoindicators. *Geochim. Cosmochim. Acta* **1988**, *52*, 2749–2765.
12. Bragin, I.V.; Zippa, E.V.; Chelnokov, G.A.; Kharitonova, N.A. Estimation of the Deep Geothermal Reservoir Temperature of the Thermal Waters of the Active Continental Margin (Okhotsk Sea Coast, Far East of Asia). *Water* **2021**, *13*, 15.

13. Chelnokov, G.; Lavrushin, V.; Bragin, I.; Kharitonova, N. Geochemistry of Thermal and Cold Mineral Water and Gases of the Tien Shan and the Pamir. *Water* **2022**, *14*, 838.
14. Fournier, R.O. Chemical Geothermometers and Mixing Models for Geothermal Systems. *Geothermics* **1977**, *5*, 41–50. https://doi.org/10.1016/0375-6505(77)90007-4.
15. Fournier, R.O. A Revised Equation for the Na–K Geothermometer. *Geotherm. Resour. Counc. Trans*. **1979**, *3*, 221–224.
16. Fournier, R.O.; Potter, R.W. Magnesium Correction to the Na–K–Ca Chemical Geothermometer. *Geochim. Cosmochim. Acta* **1979**, *43*, 1543–1550. https://doi.org/10.1016/0016-7037(79)90147-9.
17. Kharaka, Y.K.; Mariner, R.H. Chemical Geothermometers and Their Application to Formation Waters from Sedimentary Basins. In *Thermal History of Sedimentary Basins*; Springer: New York, NY, USA, 1989; pp. 99–117. https://doi.org/10.1007/978-1-4612-3492-0_6.
18. Clark, I.D. *Groundwater Geochemistry and Isotopes*, 1st ed.; CRC Press: Boca Raton, FL, USA, 2015; 456p. https://doi.org/10.1201/b18347.
19. Kendirbaeva, D.Z. Spatio-Temporal Interaction in the System "Seismicity-Thermal Waters-Solar Inhomogeneity" on the Territory of Kyrgyzstan. *Vestn. KRSU* **2019**, *19*, 110–124. https://doi.org/10.26117/2079-6641-2019-29-4-110-124. (In Russian)
20. Kendirbaeva, D.Z.; Grebennikova, V.V. On the Relationship between Geothermal Conditions and Geochemical Environment of the Kyrgyz Tien Shan. In *Deep Structure, Geodynamics, Thermal Field of the Earth, Interpretation of Geophysical Fields*; Ural Branch of Russian Academy of Sciences Publishers, Yekaterinburg, Russia, 2013; pp. 145–147. (In Russian)
21. Perelman, A.I. *Geochemistry of Elements in the Hypergenesis Zone*; Nedra: Moscow, Russia, 1972; 288p. (In Russian)
22. Klerkx, J.; Imanackunov, B. (Eds.) *Lake Issyk Kul: Its Natural Environment*; NATO Science Series: IV: Earth and Environmental Sciences; Springer: Dordrecht, The Netherlands, 2002; Volume 13. https://doi.org/10.1007/978-94-010-0491-6.
23. RD 52.24.643–2002. Method for Measuring the Mass Concentration of Ions in Samples of Natural, Drinking and Waste Waters by Ion Chromatography; Gidrometizdat: Moscow, Russia, 2002. (In Russian)
24. The European Parliament; Council of the European Union. Directive 2006/44/EC of the European Parliament and of the Council of 6 September 2006 on the Quality of Fresh Waters Requiring Protection or Improvement in Order to Support Fish Life. *Off. J. Eur. Union* **2006**, *L 264*, 20–31.
25. World Health Organization (WHO). *Guidelines for Drinking-Water Quality*, 4th ed.; Incorporating the 1st Addendum; WHO Press: Geneva, Switzerland, 2017.
26. *GOST R 54316-2020*; Natural Mineral Drinking Waters. General Specifications. Standartinform: Moscow, Russia, 2020; 44p. (In Russian)
27. Shvartsev, S.L. *Hydrogeochemistry of the Hypergenesis Zone*, 2nd ed.; Nedra: Moscow, Russia, 1998; 365p. (In Russian)
28. Davis, S.N.; Whittemore, D.O.; Fabryka-Martin, J. Uses of Chloride/Bromide Ratios in Studies of Potable Water. *Ground Water* **1998**, *36*, 338–350. https://doi.org/10.1111/j.1745-6584.1998.tb01099.x.
29. Rudnick, R.L.; Gao, S. Composition of the Continental Crust. In *The Crust*; Treatise on Geochemistry; Elsevier-Pergamon: Oxford, UK, 2003; Volume 3, pp. 1–64. https://doi.org/10.1016/B0-08-043751-6/03016-4.
30. Vinogradov, A.P. *Average Content of Chemical Elements in the Main Types of Igneous Rocks of the Earth's Crust*; Publishing House of the USSR Academy of Sciences: Moscow, Russia, 1962; 178p. (In Russian)
31. Krainov, S.R.; Ryzhenko, B.N.; Shvets, V.M. *Geochemistry of Groundwaters: Theoretical, Applied and Environmental Aspects*, 2nd ed.; TsentrLitNefteGaz: Moscow, Russia, 2012; 670p. (In Russian)

Disclaimer/Publisher's Note: The statements, opinions and data contained in all publications are solely those of the individual author(s) and contributor(s) and not of MDPI and/or the editor(s). MDPI and/or the editor(s) disclaim responsibility for any injury to people or property resulting from any ideas, methods, instructions or products referred to in the content.